World Journal of Nano Science and Engineering, 2014, 4, 21-28
Published Online March 2014 in SciRes. http://www.scirp.org/journal/wjnse
http://dx.doi.org/10.4236/wjnse.2014.41004

Scientific Research

X-Ray Analysis by Williamson-Hall and Size-Strain Plot Methods of ZnO Nanoparticles with Fuel Variation

Yendrapati Taraka Prabhu[1*], Kalagadda Venkateswara Rao[1], Vemula Sesha Sai Kumar[1], Bandla Siva Kumari[2]

[1]Centre for Nano Science and Technology, IST, Jawaharlal Nehru Technological University, Hyderabad, India
[2]Botany Department, Andhra Loyola College, Vijayawada, India
Email: [*]prabusj@gmail.com

Received 6 November 2013; revised 9 December 2013; accepted 16 December 2013

Abstract

In this paper, a simple and facile surfactant assisted combustion synthesis is reported for the ZnO nanoparticles. The synthesis of ZnO-NPs has been done with the assistance of non-ionic surfactant TWEEN 80. The effect of fuel variations and comparative study of fuel urea and glycine have been studied by using characterization techniques like X-ray diffraction (XRD), transmission electron microscope (TEM) and particle size analyzer. From XRD, it indicates the presence of hexagonal wurtzite structure for ZnO-NPs. Using X-ray broadening, crystallite sizes and lattice strain on the peak broadening of ZnO-NPs were studied by using Williamson-Hall (W-H) analysis and size-strain plot. Strain, stress and energy density parameters were calculated for the XRD peaks of all the samples using (UDM), uniform stress deformation model (USDM), uniform deformation energy density model (UDEDM) and by the size-strain plot method (SSP). The results of mean particle size showed an inter correlation with W-H analysis, SSP, particle analyzer and TEM results.

Keywords

Surfactant Assisted Combustion; X-Ray Diffraction (XRD); Transmission Electron Microscope (TEM); Particle Analyzer

1. Introduction

In many areas of chemistry, physics and material science transition metal oxides with nano structure have at-

[*]Corresponding author.

How to cite this paper: Prabhu, Y.T., Rao, K.V., Kumar, V.S.S. and Kumari, B.S. (2014) X-Ray Analysis by Williamson-Hall and Size-Strain Plot Methods of ZnO Nanoparticles with Fuel Variation. *World Journal of Nano Science and Engineering*, **4**, 21-28.
http://dx.doi.org/10.4236/wjnse.2014.41004

tracted substantial interest during the last few years because of their novel optical and electrical properties as well as semiconductor crystals with a large binding energy (60 meV) [1]. In a variety of applications, Zinc oxide nanoparticles are used as photocatalyst [2], catalyst [3], antibacterial treatment [4] and UV absorption. Various physical methods such as vapor phase transparent process [5], pulse laser deposition [6] [7], vapor transparent deposition and chemical vapor deposition [8] have been developed for preparation of nano ZnO. These days, Sol-gel method is one of the known procedures for the preparation of metal oxide nanoparticles [9] which is based on the hydrolysis of reactive metal precursor.

Deviations from perfect crystallinity extend infinitely in all directions which lead to broadening of the diffraction peaks. The crystallite size and lattice strain are the two main properties which could be extracted from the peak width analysis. Due to the formation of polycrystalline aggregates [10], the crystallite size of the particle is not the same as the particle size. The crystal imperfections could be measured from the distributions of lattice constants. The basis of strain also includes contact or sinter stress, grain boundary, triple junction, stacking faults and coherency stress [11]. In different ways, Bragg peak is affected by crystallite size and lattice strain which increase the peak width and intensity shifting the 2θ peak position accordingly. The crystallite size varies as $1/\cos\theta$ and stain varies as $\tan\theta$ from the peak width. The size and strain effects on peak broadening are known from the above difference of 2θ. W-H analysis is an integral breadth method. Size-induced and strain-induced broadenings are known by considering the peak width as a function of 2θ [12].

In this paper firstly, a simple method for the synthesis of ZnO-NPs by surfactant assisted combustion synthesis is disused. It was found that this method is a quick, mild, energy-efficient and eco-friendly route to producing ZnO nanoparticles. Secondly, comparative studies of the mean particle size of ZnO-NPs from TEM measurements and from the powdered XRD are dealt with. Using William Hall modified form strain, uniform deformation model (UDM), uniform stress deformation model (USDM), uniform deformation energy-density model (UDEDM) and the size-strain plot method (SSP) provided information on the stress-strain relation, and the strain ε as a function of energy density (u) was estimated.

2. Experimental Details

2.1. Instrumentation

The crystal phases of the synthesized powders were determined by X-ray diffraction (XRD, Bruker D & Advance, Germany) using CuKα as radiation source (40 kV, step size 0.02, scan rate 0.5 min^{-1}, $20^\circ \le 2\theta \le 80^\circ$). The particle size is measured by Nano Particle Size Analyzer (SZ-100 Nanoparticle, Horiba, Germany). The surface morphology of ZnO nanoparticles were studied with transmission electron microscope (Tecnai 20 T G2 (FEI)).

2.2. Preparation of ZnO Nanoparticles

The starting materials such as zinc nitrate and non-ionic surfactant are taken in same amounts for both the samples and thus changing the fuels glycine and urea. Freshly prepared aqueous solutions of the chemicals were used for the synthesis of nanoparticles. At room temperature the chemicals are added one by one with the 0.1 M solution of zinc nitrate, 0.15 M solution of glycine for first sample and urea for the second sample with 0.025 M solution of non-ionic surfactant. The mixture of chemicals was then heated on a hot plate in separate beakers which led the chemical mixture to self-combustion. After combustion the final precipitate is subjected to calcinations for 1 hr at 400˚C. Thus we successfully obtained a pure ZnO nano powders for different fuels in this synthesis.

3. Results and Discussion

3.1. XRD

Figure 1 shows the XRD patterns of as-syntheised ZnO nanoparticles by surfactant assisted combustion with fuels glycine and urea. All the diffraction peaks can be assigned to hexagonal phase with Wurtzite structure with space group (P63mc), JCPDS card No.36-1415 and unit cell parameters a = b = 0.3249 nm and c = 0.5206 nm. The crystallite size is calculated from full width at half maximum (FWHM) of the peaks (1 0 0) (0 0 2) (1 0 1) (1 0 2) (1 1 0) (1 0 3) (1 1 2) and (2 0 1). The Bragg peak breadth is a combination of both instrument- and sample

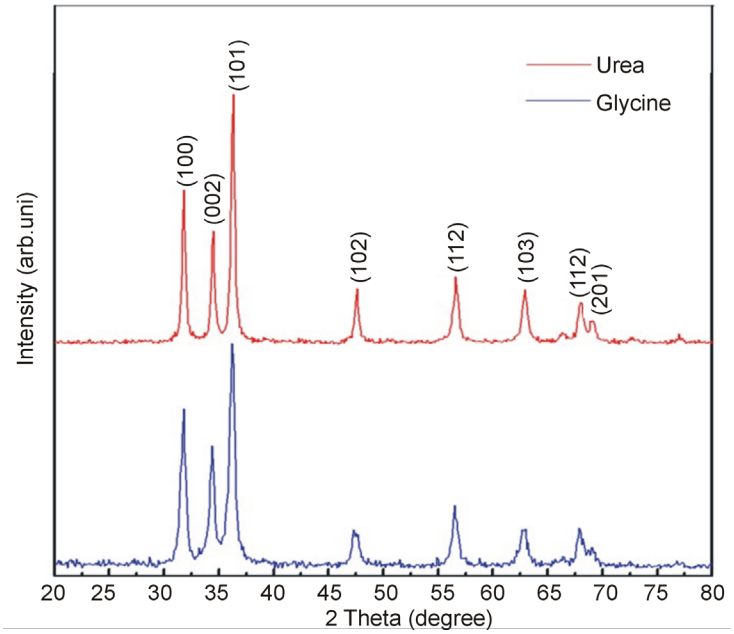

Figure 1. The XRD pattern for the nano ZnO with fuels Gylcine and urea.

dependent effects. To remove these aberrations, it is needed to assemble a diffraction pattern from the line broadening of a standard material such as silicon to determine the instrumental broadening. The instrument-corrected broadening [13] β_D corresponding to the diffraction peak of ZnO was estimated using the relation. The lattice constants of ZnO with varied fuels are given in the **Table 1**.

$$\beta_D^2 = \left[\beta_{\text{measures}}^2 - \beta_{\text{instrumental}}^2\right] \tag{1}$$

$$D = \frac{k\lambda}{\beta_D \cos\theta} \Rightarrow \cos\theta \frac{k\lambda}{D}\left(\frac{1}{\beta_D}\right) \tag{2}$$

3.2. Williamson-Hall Methods

Crystal imperfections and distortion of strain-induced peak broadening are related by $\varepsilon \approx \beta_s/\tan\theta$. There is an extraordinary property of Equation (2) which has the dependency on the diffraction angle θ. Scherrer-equation follows a $1/\cos\theta$ dependency but not $\tan\theta$ as W-H method. This basic difference was that both microstructural causes small crystallite size and microstrain occur together from the reflection broadening. Depending on different θ positions the separation of size and strain broadening analysis is done using Williamson and Hall. The following results are the addition of the Scherrer equation and $\varepsilon \approx \beta_s/\tan\theta$.

$$\beta_{hkl} = \beta_S + \beta_D \tag{3}$$

$$\beta_{hkl} = \left(\frac{k\lambda}{D\cos\theta}\right) + 4\varepsilon\tan\theta \tag{4}$$

Rearranging Equation (4) gives:

$$\beta_{hkl} = \left(\frac{k\lambda}{D}\right) + 4\varepsilon\sin\theta \tag{5}$$

Here Equation (5) stands for UDM where it is assumed that stain is uniform in all crystallographic directions. $\beta\cos\theta$ was plotted with respect to $4\sin\theta$ for the peaks of ZnO with varied fuels. Strain and particle size are calculated from the slope and y-intercept of the fitted line respectively. From the lattice parameters calculations it was observed that this strain might be due to the lattice shrinkage. The UDM analysis results are shown in **Figure 2**.

Table 1. The structure parameters of ZnO nanoparticles with fuels glycine and urea.

Fuel	Unit Cell Parameters/nm		Cell Volume (nm^3)	Size (nm)	c/a ratio
	a	c			
Glycine	3.252	5.214	47.755	12.89	1.6032
Urea	3.252	5.208	47.701	36.77	1.6015

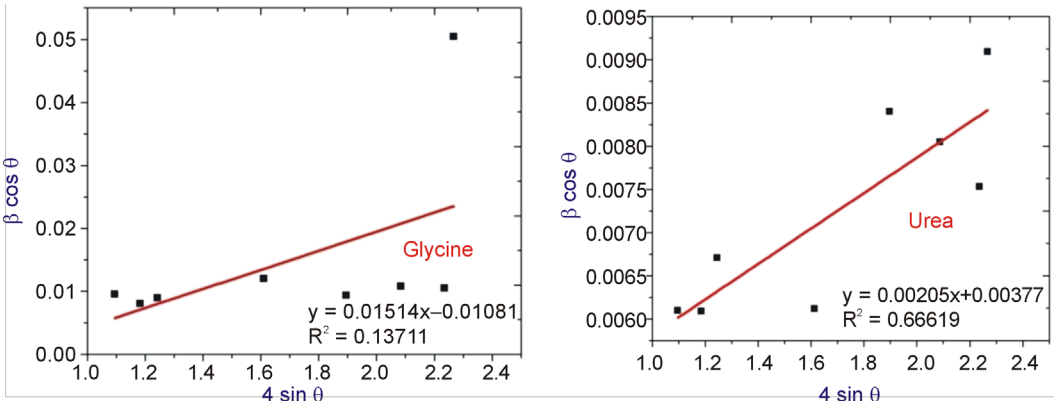

Figure 2. The W-H analysis of ZnO nanoparticles with fuels glycine and urea assuming UDM. Fit to the data, the strain is extracted from the slope and the crystalline size is extracted from the y-intercept of the fit.

From Uniform Stress Deformation Model (USDM) strain is calculated from the Hook's Law maintaining linea proportionality between stress and strain by $\sigma = Y\varepsilon$, where σ is the stress and Y is the Young's modulus. This Hook's law is valid for a significantly small strain. Supposing a small strain to be present in the ZnO with varied fuels, Hooke's law can be used here. Applying the Hooke's law approximation to Equation (5) yields:

$$\beta_{hkl}\cos\theta = \left(\frac{k\lambda}{D}\right) + \left(\frac{4\sigma\sin\theta}{Y_{hkl}}\right) \tag{6}$$

For a hexagonal crystal, Young's modulus is given by the following relation [11] (Equation (7)). where S_{11}, S_{13}, S_{33}, S_{44} are the elastic compliances of ZnO with values of 7.858×10^{-12}, -2.206×10^{-12}, 6.940×10^{-12}, 23.57×10^{-12} $m^2 \cdot N^{-1}$, respectively [11]. Young's modulus, Y, for hexagonal ZnO was calculated as ≈130 GPa. $4\sin\theta/Y_{hkl}$ and $\beta\cos\theta$ were taken on x-axis and y-axis respectively. The USDM plots for ZnO with varied fuels are shown in the **Figure 3**. The stress is calculated from the slope.

$$Y_{hkl} = \left(\frac{\left[h^2 + \frac{(h+2k)^2}{3} + \frac{(al)^2}{c} \right]^2}{S_{11}\left(h^2 + \frac{(h+2k)^2}{3} \right)^2 + S_{33}\left(\frac{al}{c} \right)^4 + (2S_{13} + S_{44})\left(h^2 + \frac{(h+2k)^2}{3}\left(\frac{al}{c} \right)^2 \right)} \right) \tag{7}$$

The energy density of a crystal was calculated from a model called Uniform Deformation Energy Density Model (UDEDM). From Equation (8) we need to implicit that crystals are to be homogeneous and isotropic nature. The energy density u can be calculated from $u = \left(\varepsilon^2 Y_{hkl}\right)/2$ using Hooke's law. The Equation (8) can be modified according the energy and strain relation.

$$\beta_{hkl} = \left(\frac{k\lambda}{D}\right) + \left(4\sin\theta\left(\frac{2u}{Y_{hkl}}\right)^{1/2}\right) \tag{8}$$

$4\sin\theta\left(2u/Y_{hkl}\right)^{1/2}$ and $\beta_{hkl}\cos\theta$ were taken on x-axis and y-axis respectively. From the slope the anisotropic energy density u was calculated and the crystallite size D from the Y-intercept from **Figure 4**. We know that $\sigma = \varepsilon Y$ and $u = \left(\varepsilon^2 Y_{hkl}\right)/2$ the stress σ was calculated as $u = \left(\varepsilon^2 Y_{hkl}\right)/2$.

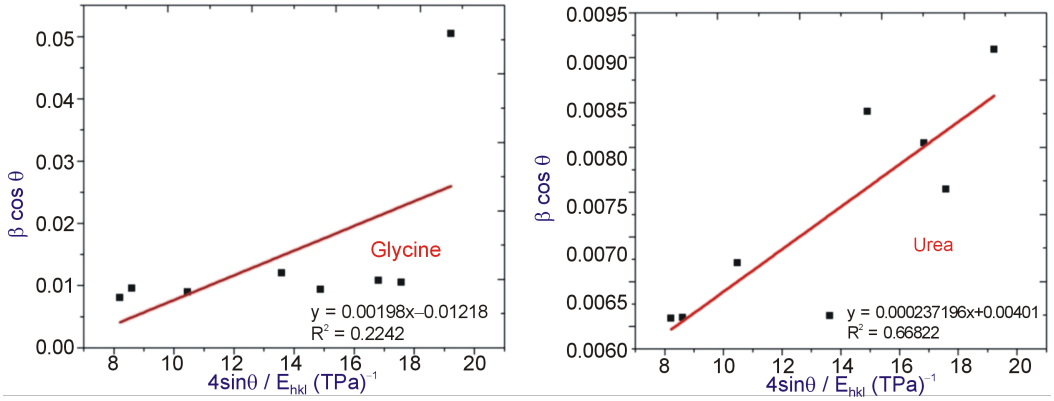

Figure 3. The modified form of W-H analysis assuming USDM for ZnO with fuels glycine and urea. Fit to the data, the stress is extracted from the slope and the crystalline size is extracted from the y-intercept of the fit.

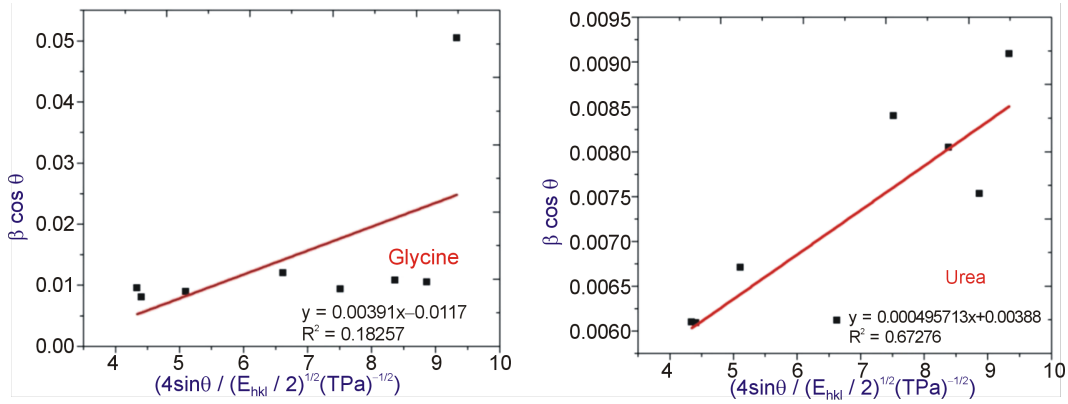

Figure 4. The modified form of W-H analysis assuming UDEDM for ZnO with fuels glycine and urea. Fit to the data, the density of energy is extracted from the slope and the crystalline size is extracted from the y-intercept of the fit.

3.3. Size-Strain Plot Method

Williamson-Hall plot has illustrated that line broadening was basically isotropic. Due to microstrain contribution the diffracting domains were isotropic. Size-strain parameters can be obtained from the "size-strain plot" (SSP). This has a benefit that less importance is given to data from reflections at high angles. In this estimation, it is assumed that profile is illustrated by "strain profile" by a Gaussian function and the "crystallite size" by Lorentzian function [14]. Hence we have

$$\left(d_{hkl}\beta_{hkl}\cos\theta\right)^2 = \frac{k}{D}\left(d_{hkl}^2\beta_{hkl}\cos\theta\right) + \left(\frac{\varepsilon}{2}\right)^2 \tag{9}$$

where k is a constant, shape of the particles for spherical particles it is given as 3/4. In **Figure 5**, $d_{hkl}^2\beta_{hkl}\cos\theta$ and $\left(d_{hkl}\beta_{hkl}\cos\theta\right)^2$ were taken on x-axis and y-axis respectively for all peaks of ZnO-NPs with the wurtzite hexagonal phase from $2\theta = 20^\circ$ to $2\theta = 80^\circ$. The particle size is calculated from the slope linearly fitted data and the root of the y-intercept gives the strain.

3.4. TEM Method

From TEM results size and morphology of ZnO particles are analyzed and represented in **Figures 6** and **7**. Image reveals that the samples are with the average size of 20 - 30 nm which is in good agreement with that estimated by Scherer formula. In the **Table 2** the results attained from Scherrer method, UDM, USDM, UDEDM, SSP models and TEM are summarized. SAED pattern is shown in **Figure 8**.

Table 2. Geometric parameters of ZnO nanoparticles with fuels glycine and urea.

Fuel	Williamsom-Hall Method									Size-Strain Plot Method			
	UDM		USDM			UDEDM							
	D	*ε* no	*D*	*ε* no	*σ*	*D*	*ε* no	*σ*	*u*	*D*	*ε* no	*σ*	*u*
	(nm)	Unit × 10^{-3}	(nm)	Unit × 10^{-3}	(Mpa)	(nm)	Unit × 10^{-3}	(Mpa)	(kJm^{-3})	(nm)	Unit × 10^{-3}	(Mpa)	(kJm^{-3})
Glycine	12.82	1.51	11.37	1.77	168.24	11.84	1.84	198.21	81.3	12.14	1.808	199.35	92.54
UREA	36.75	0.205	34.56	0.212	123.54	35.72	0.9422	136.71	53.1	35.86	0.439	139.24	52.69

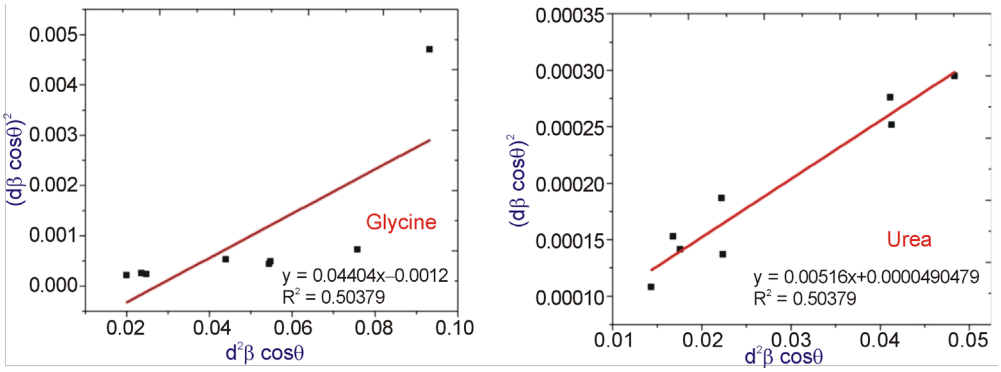

Figure 5. The SSP plot of ZnO with fuels glycine and urea. The particle size is achieved from the slop of the liner fitted data and the root of y-intercept gives the strain.

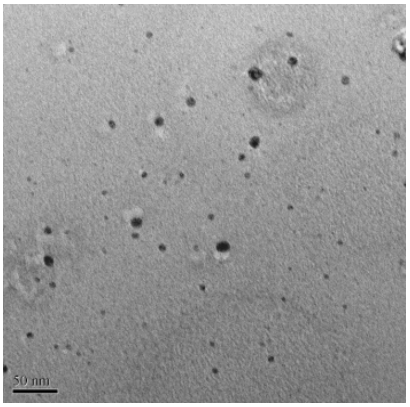

Figure 6. TEM micrographs of ZnO nanoparticles with fuel glycine.

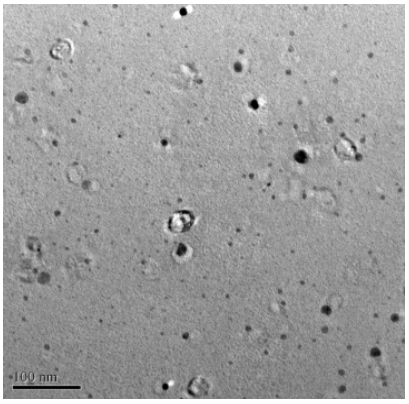

Figure 7. TEM micrographs of ZnO nanoparticles with fuel urea.

3.5. Particle Analyzer

Using Nano Particle Analyzer (SZ100) the size of the nanopowders is measured. The average particle sizes for samples with fuels glycine and urea are shown with histogram in **Figures 9** and **10**. All the results from particle analyzer are in good agreement with the XRD results of crystallite sizes.

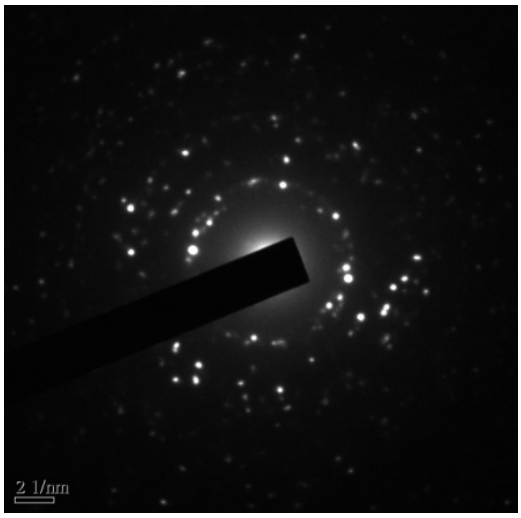

Figure 8. SAED pattern of ZnO.

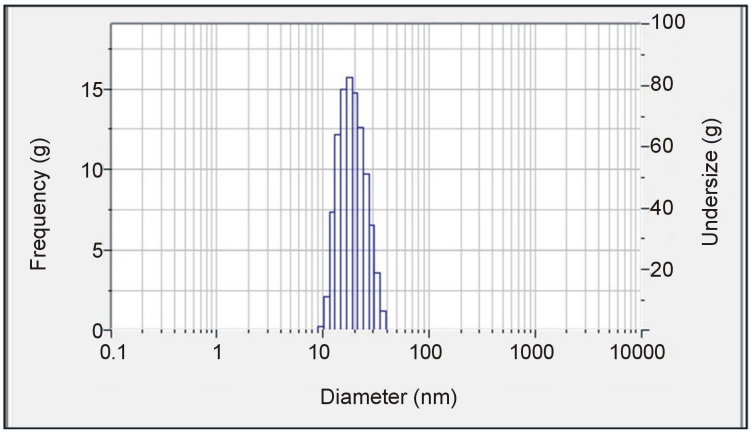

Figure 9. Particle analyzer histograms of fuel glycine of ZnO powders.

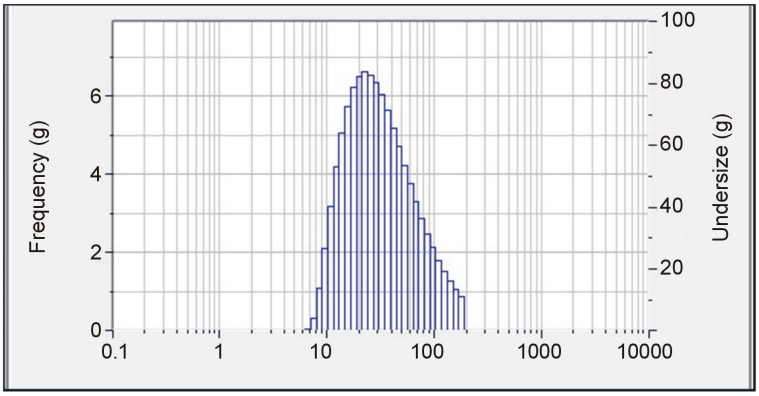

Figure 10. Particle analyzer histograms of fuel urea of ZnO powders.

4. Conclusion

In summary, we have successfully synthesized porous nanocrystalline ZnO powder by novel surfactant assisted combustion method. Systematic variation of fuels resulted in nanoparticles of the smallest size of crystallite size 12.82 nm and 36.42 nm for glycine and urea fuels respectively which were in good agreement with TEM results. When the crystallite size decreased for sample with fuel glycine cell volume, c/a ratio and micro strain increased. Similarly as the crystallite size increased for sample with fuel urea cell volume, c/a ratio and micro strain decreased. This broadening was analyzed by the Scherrer formula, modified forms of W-H analysis and the size-strain plot method. From the results, it was observed that the strain value decreased but the particle size increased as doping concentration increased. The TEM results were in good agreement with the results of the W-H and the SSP methods.

References

[1] Hu, J.T., Odom, T.W. and Liebe, C.M. (1999) Chemistry and Physics in One Dimension: Synthesis and Properties of Nanowires and Nanotubes. *Accounts of Chemical Research*, **32**, 435-445. http://dx.doi.org/10.1021/ar9700365

[2] Annapoorani, R., Dhananjeyan, M.R. and Renganathan, R. (1997) An Investigation on ZnO Photocatalysed Oxidation of Uracil. *Journal of Photochemistry and Photobiology A*: *Chemistry*, **111**, 215-221. http://dx.doi.org/10.1016/S1010-6030(97)00170-6

[3] Huang, W.-J., Fang, G.-C. and Wang, C.-C. (2005) A Nanometer-ZnO Catalyst to Enhance the Ozonation of 2,4,6-Trichlorophenol in Water. *Colloids and Surfaces A*: *Physicochemical and Engineering Aspects*, **260**, 45-51. http://dx.doi.org/10.1016/j.colsurfa.2005.01.031

[4] Sánchez, L., Peral, J. and Domènech, X. (1996) Degradation of 2,4-Dichlorophenoxyacetic Acid by *in Situ* Photogenerated Fenton Reagent. *Electrochimica Acta*, **41**, 1981-1985. http://dx.doi.org/10.1016/0013-4686(95)00486-6

[5] Chen, B.J., Sun, X.W., Xu, C.X. and Tay, B.K. (2004) Growth and Characterization of Zinc Oxide Nano/Micro-Fibers by Thermal Chemical Reactions and Vapor Transport Deposition in Air. *Physica E*, **21**, 103-107. http://dx.doi.org/10.1016/j.physe.2003.08.077

[6] Nakata, Y., Okada, T.and Maeda, M. (2002) Deposition of ZnO Film by Pulsed Laser Deposition at Room Temperature. *Applied Surface Science*, **197**, 368-370. http://dx.doi.org/10.1016/S0169-4332(02)00426-9

[7] Yoo, Y.-Z., Jin, Z.-W., Chikyow, T., Fukumura, T., Kawasaki, M. and Koinuma, H. (2012) S Doping in ZnO Film by Supplying ZnS Species with Pulsed-Laser-Deposition Method. *Applied Physics Letters*, **81**, 3798. http://dx.doi.org/10.1063/1.1521577

[8] Li, Y.J., Duan, R., Shi, P.B. and Qin, G.G. (2004) Synthesis of ZnO Nanoparticles on Si Substrates Using a ZnS Source. *Journal of Crystal Growth*, **260**, 309-315. http://dx.doi.org/10.1016/j.jcrysgro.2003.08.041

[9] Yang, X.-L., Dai, W.-L., Chen, H., Cao, Y., Li, H.X., He, H.Y. and Fan, K.N. (2004) Novel Efficient and Green Approach to the Synthesis of Glutaraldehyde over Highly Active W-Doped SBA-15 Catalyst. *Journal of Catalysis*, **229**, 259-263. http://dx.doi.org/10.1016/j.jcat.2004.10.009

[10] Ramakanth, K. (2007) Basic of Diffraction and Its Application. I.K. International Publishing House Pvt. Ltd., New Dehli.

[11] Zhang, J.-M., Zhang, Y., Xu, K.-W. and Ji, V. (2006) General Compliance Transformation Relation and Applications for Anisotropic Hexagonal Metals. *Solid State Communications*, **139**, 87-91. http://dx.doi.org/10.1016/j.ssc.2006.05.026

[12] Suranarayana, C. and Norton, M.G. (1998) X-Ray Diffraction: A Practical Approach. Springer, New York. http://dx.doi.org/10.1007/978-1-4899-0148-4

[13] Rogers, K.D. and Daniels, P. (2002) An X-Ray Diffraction Study of the Effects of Heat Treatment on Bone Mineral Microstructure. *Biomaterials*, **23**, 2577-2585. http://dx.doi.org/10.1016/S0142-9612(01)00395-7

[14] Nye, J.F. (1985) Physical Properties of Crystals: Their Representation by Tensors and Matrices. Oxford, New York.